crystals

MDPI

Article

Pseudo-Spin Polarized One-Way Elastic Wave Eigenstates in One-Dimensional Phononic Superlattices

Pierre A. Deymier [1,*,†], Keith Runge [1,†], Alexander Khanikaev [2,3,†] and Andrea Alù [3,4,†]

[1] Department of Materials Science and Engineering, University of Arizona, Tucson, AZ 85721, USA; krunge@arizona.edu
[2] Department of Electrical Engineering, The City College of New York, New York, NY 10031, USA; akhanikaev@ccny.cuny.edu
[3] Physics Program, Graduate Center, City University of New York, New York, NY 10016, USA; aalu@gc.cuny.edu
[4] Photonics Initiative, Advanced Science Research Center, City University of New York, New York, NY 10031, USA
* Correspondence: deymier@arizona.edu
† Current affiliation: New Frontiers of Sound Science and Technology Center, The University of Arizona, Tucson, AZ 85721, USA.

Abstract: We investigate a one-dimensional discrete binary elastic superlattice bridging continuous models of superlattices that showcase a one-way propagation character, as well as the discrete elastic Su–Schrieffer–Heeger model, which does not exhibit this character. By considering Bloch wave solutions of the superlattice wave equation, we demonstrate conditions supporting elastic eigenmodes that do not satisfy the translational invariance of Bloch waves over the entire Brillouin zone, unless their amplitude vanishes for a certain wave number. These modes are characterized by a pseudo-spin and occur only on one side of the Brillouin zone for a given spin, leading to spin-selective one-way wave propagation. We demonstrate how these features result from the interplay of the translational invariance of Bloch waves, pseudo-spins, and a Fabry–Pérot resonance condition in the superlattice unit cell.

Keywords: phononic superlattice; pseudo spin; one-way propagation; topological acoustics

Citation: Deymier, P.A.; Runge, K.; Khanikaev, A.; Alù, A. Pseudo-Spin Polarized One-Way Elastic Wave Eigenstates in One-Dimensional Phononic Superlattices. *Crystals* **2024**, *14*, 92. https://doi.org/10.3390/cryst14010092

Academic Editor: Yuri Kivshar

Received: 15 December 2023
Revised: 11 January 2024
Accepted: 13 January 2024
Published: 19 January 2024

1. Introduction

Breaking reciprocity is one principle for forming acoustic or elastic waves traveling only in one direction (that is, one-way wave propagation). A variety of mechanisms can be used to break reciprocity, which range from symmetry breaking to exploiting non-linearity and spatiotemporal modulations [1,2]. For example, breaking time-reversal symmetry by using gyroscopic inertial effects in lattice structures can lead to the topologically protected one-way propagation of elastic waves localized at the edges of the lattice [3]. The dependence on the amplitude of the dynamic behavior of the non-linear waves may also lead to non-reciprocity [4]. Moreover, the modulation in space and time of the physical properties of elastic media introduces a bias that breaks time-reversal symmetry and subsequently reciprocity, leading to the one-way propagation of bulk elastic waves [5–7].

While breaking reciprocity is one route to one-way propagation [8,9], other topologically protected systems that preserve reciprocity have been demonstrated. For example, static one-dimensional superlattices that do not break time-reversal symmetry and obey linear elasticity have been shown to support robust, topologically protected elastic eigenwaves with non-zero amplitude in the forward propagation direction but with zero amplitude in the opposite direction [10]. These one-way-propagating, topologically protected eigenwaves occur along elastic bands with a non-zero Berry phase. Due to time-reversal symmetry, these eigenwaves possess a pseudo-spin that breaks mirror symmetry, and an

eigenwave with opposite handedness is expected to be supported by the system in the reverse propagation direction. Hence, differing from non-reciprocal one-way systems, these responses do not generally isolate but can be used to efficiently direct signals towards desired directions and are robust against back-reflections, as long as disorder or defects do not couple the two pseudo-spin hands.

Here, we develop a model for one-dimensional discrete phononic superlattices, which enables us to bridge continuum superlattices that support reciprocal one-way eigenwaves and the elastic analogue of the well-known one-dimensional Su–Schrieffer–Heeger (SSH) model [11,12], which does not generally support topologically protected, one-way-propagating bulk waves. The discrete superlattice model is investigated using the transfer matrix method to calculate its band structure and corresponding eigenmodes. We show that the transfer matrix exhibits, under specific conditions, eigenvalues that do not span the complete unit circle in the complex plane. Subsequently, such eigenmodes do not satisfy the translational invariance of the elastic modes in the form of Bloch waves over the entire Brillouin zone, unless their amplitude vanishes for a certain wave number. This condition occurs on one side of the Brillouin zone and not the other, leading to one-way wave propagation. In the case of the continuous limit of a finite superlattice, we show that reciprocity is obeyed, as expected, and the one-way nature is associated with an inherent handedness of the eigenmodes (pseudo-spin), which breaks the mirror symmetry. One-way propagation is identified as the combined effect of translational invariance, pseudo-spin, and Fabry–Pérot resonances [13] in one of the constitutive media of the superlattice. These results offer an original view of unidirectional propagation, which can be probed via exciting one-way modes by spin-selective sources in 1D periodic systems.

2. Model and Method

2.1. Model System and Dynamic Equations of Motion

The binary superlattice system under study is formed by periodically repeating unit cells composed of two segments of different one-dimensional mass–spring harmonic chains (see Figure 1). Each mass is identical and equals 1; the stiffness levels of the springs in segments 1 and 2 equal K_1 and K_2, respectively; and the spacing between adjacent masses equals a. The lengths of the segments are $d_1 = na$ and $d_2 = pa$, where n and p are integers. Segments 1 and 2 are separated by interfaces labelled I and II. In this model, we assume that the stiffness of the springs (bond strength) in a segment remains the same up to the interfaces. When $n = 1$ and $p = 1$, the system becomes the Su–Schrieffer–Heeger (SSH) model [12]. For large values of n and p, in the long wavelength limit, the system approaches a continuous superlattice.

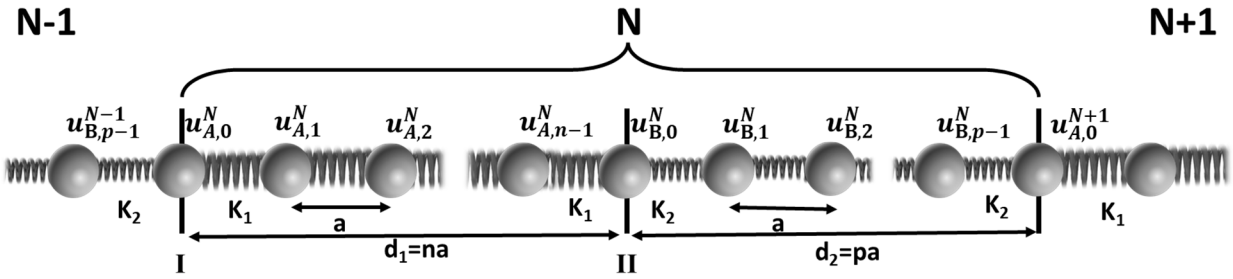

Figure 1. Schematic representation of a one-dimensional discrete superlattice. A periodically repeating unit cell N is composed of equally spaced identical unit masses coupled through linear springs with stiffnesses of K_1 and K_2. See text for more details.

The displacement of a mass, $m \in [0, n-1]$, in segment 1 of unit cell N is defined as $u^N_{A,m}$. Similarly, the displacement of masses in segment 2 of unit cell N is labelled $u^N_{B,l}$,

with $l \in [0, p-1]$. The masses obey bulk equations of motion in segments 1 and 2 for $m \in [1, n-2]$ and $l \in [1, p-2]$, namely:

$$\frac{d^2u^N_{A,m}}{dt^2} = K_1\left(u^N_{A,m+1} - u^N_{A,m}\right) - K_1\left(u^N_{A,m} - u^N_{A,m-1}\right) \tag{1a}$$

$$\frac{d^2u^N_{B,l}}{dt^2} = K_2\left(u^N_{B,l+1} - u^N_{B,l}\right) - K_2\left(u^N_{B,l} - u^N_{B,l-1}\right) \tag{1b}$$

Equation (1a,b) supports plane wave solutions of the form:

$$u^N_{A,m} = \left(A^N_+ e^{ik_1 ma} + A^N_- e^{-ik_1 ma}\right)e^{i\omega t} \tag{2a}$$

$$u^N_{B,l} = \left(B^N_+ e^{ik_2 la} + B^N_- e^{-ik_2 la}\right)e^{i\omega t} \tag{2b}$$

The wave number k_j with $j = 1, 2$ is related to the angular frequency via the well-known dispersion relation of infinite harmonic chains:

$$\omega^2 = 4K_i\left(\sin k_j \frac{a}{2}\right)^2 \tag{3}$$

The behavior of the superlattice will, therefore, be dependent on the overlap of the bulk bands (density of states) of the materials forming segments 1 and 2.

Since the system is periodic with period $L = d_1 + d_2$, we consider Bloch wave solutions, i.e., we choose $A^N_\pm = e^{iqNL}A_\pm$ and $B^N_\pm = e^{iqNL}B_\pm$, where q is the wave number. We remove the upper script N on $A_\pm$ and $B_\pm$ when the periodicity is explicitly accounted for in the plane wave term e^{iqNL}.

The equations of the motion of masses at interfaces I and II are as follows:

$$\frac{d^2u^N_{A,0}}{dt^2} = K_1\left(u^N_{A,1} - u^N_{A,0}\right) - K_2\left(u^N_{A,0} - u^{N-1}_{B,p-1}\right) \tag{4a}$$

$$\frac{d^2u^N_{B,0}}{dt^2} = K_2\left(u^N_{B,1} - u^N_{B,0}\right) - K_1\left(u^N_{B,0} - u^N_{A,n-1}\right) \tag{4b}$$

Inserting the null terms $-K_1\left(u^N_{A,0} - u^{N-1}_{A,p-1}\right) \mp K_1\left(u^N_{A,0} - u^{N-1}_{A,p-1}\right)$ into Equation (4a) and $-K_2\left(u^N_{B,0} - u^N_{B,-1}\right) \mp K_2\left(u^N_{B,0} - u^N_{B,-1}\right)$ into Equation (4b), we obtain, by virtue of the bulk equations of motion, the conditions of the continuity of forces at interfaces I and II:

$$K_1\left(u^N_{A,0} - u^{N-1}_{A,p-1}\right) = K_2\left(u^N_{A,0} - u^{N-1}_{B,p-1}\right) \tag{5a}$$

$$K_2\left(u^N_{B,0} - u^N_{B,-1}\right) = K_1\left(u^N_{B,0} - u^N_{A,n-1}\right) \tag{5b}$$

We also introduce the following conditions of the continuity of displacement at I and II:

$$u^N_{A,0} = u^{N-1}_{B,p} \tag{6a}$$

$$u^N_{B,0} = u^N_{A,n} \tag{6b}$$

With these conditions, Equation (5a,b) becomes:

$$K_1\left(u^N_{A,0} - u^N_{A,-1}\right) = K_2\left(u^{N-1}_{B,p} - u^{N-1}_{B,p-1}\right) \tag{7a}$$

$$K_2\left(u^N_{B,0} - u^N_{B,-1}\right) = K_1\left(u^N_{A,n} - u^N_{A,n-1}\right) \tag{7b}$$

In Equation (7a), we use $u^{N-1}_{A,p-1} = u^{N}_{A,-1}$. Inserting the general solutions given by Equation (2a,b) and the Bloch wave form into Equations (6a,b) and (7a,b) yields the following set of dynamic equations:

$$\begin{pmatrix} \alpha_1 & \beta_1 & -1 & -1 \\ f\alpha_1\delta_-^{(1)} & f\beta_1\delta_+^{(1)} & -\delta_-^{(2)} & -\delta_+^{(2)} \\ 1 & 1 & -e^{-iqL}\alpha_2 & -e^{-iqL}\beta_2 \\ f\delta_-^{(1)} & f\delta_+^{(1)} & -e^{-iqL}\alpha_2\delta_-^{(2)} & -e^{-iqL}\beta_2\delta_+^{(2)} \end{pmatrix} \begin{pmatrix} A_+ \\ A_- \\ B_+ \\ B_- \end{pmatrix} = 0 \tag{8}$$

where $f = \frac{K_1}{K_2}$, $\alpha_1 = \frac{1}{\beta_1} = e^{ik_1na}$, $\alpha_2 = \frac{1}{\beta_2} = e^{ik_2pa}$, and $\delta_\pm^{(j)} = 1 - e^{\pm ik_ja}$, with $j = 1, 2$. We also enforce the periodicity of the system, requiring that the solutions in Equation (2a,b) take the form of Bloch waves; that is, $B_\pm^{N-1} = B_\pm^N e^{-iqL}$.

Equation (8) possesses non-trivial solutions when the determinant of the dynamic matrix is equal to zero. This condition leads to the dispersion relation:

$$\begin{gathered} f\left(\delta_+^{(2)} - \delta_-^{(2)}\right)\left(\delta_+^{(1)} - \delta_-^{(1)}\right)2\cos qL - (\alpha_1\beta_2 + \beta_1\alpha_2)\left(\delta_+^{(2)} - f\delta_+^{(1)}\right)\left(\delta_-^{(2)} - f\delta_-^{(1)}\right) + (\alpha_1\alpha_2 + \beta_1\beta_2) \\ \left(\delta_+^{(2)} - f\delta_-^{(1)}\right)\left(\delta_-^{(2)} - f\delta_+^{(1)}\right) = 0. \end{gathered} \tag{9}$$

This dispersion relation can be reformulated as:

$$\cos qL = \cos k_1d_1\cos k_2d_2 + \left[-\frac{1}{2}\left(\frac{1}{f}\frac{4\left(\sin k_2\frac{a}{2}\right)^2}{\sin k_1a\sin k_2a} + f\frac{4\left(\sin k_1\frac{a}{2}\right)^2}{\sin k_1a\sin k_2a}\right) + \frac{4\left(\sin k_1\frac{a}{2}\right)^2\left(\sin k_2\frac{a}{2}\right)^2}{\sin k_1a\sin k_2a}\right]\sin k_1d_1\sin k_2d_2 \tag{10}$$

2.2. SSH Limit

In the SSH scenario ($n = p = 1$), $\sin k_1d_1\sin k_2d_2 = \sin k_1a\sin k_2a$ and $\cos k_1d_1\cos k_2d_2 = \cos k_1a\cos k_2a$. Using the dispersion relations given by Equation (3) and basic trigonometric relations, Equation (10) reduces to:

$$\omega^4 - 2(K_1 + K_2)\omega^2 + 2K_1K_2(1 - \cos qL) = 0 \tag{11}$$

This leads to the usual SSH dispersion relation:

$$\omega^2 = K_1 + K_2 \pm \sqrt{K_1^2 + K_2^2 + 2K_1K_2\cos qL} \tag{12}$$

Equation (8) can be manipulated algebraically to obtain a relationship between $A = A_+ + A_-$ and $B = B_+ + B_-$, namely:

$$A\left(-\omega^2 + K_1 + K_2\right) = \left(K_1 + K_2e^{-iqL}\right)B \tag{13}$$

The amplitudes $A = A_+ + A_-$ and $B = B_+ + B_-$ do not differentiate between positive or negative k_j, since $m = 0$ and $l = 0$ in Equation (2a,b).

Employing Equation (12) in the form of $\left(-\omega^2 + K_1 + K_2\right)^2 = \left(K_1 + K_2e^{-iqL}\right)\left(K_1 + K_2e^{+iqL}\right)$, we recover the complex SSH amplitudes [14]:

$$\begin{pmatrix} A \\ B \end{pmatrix} \propto \begin{pmatrix} \sqrt{K_1 + K_2e^{-iqL}} \\ \sqrt{K_1 + K_2e^{+iqL}} \end{pmatrix} \tag{14}$$

The dispersion relation (Equation (12)) exhibits band inversion when varying the spring stiffness. The complex amplitudes (Equation (14)) support a non-conventional topology over the Brillouin zone, $q \in \left[-\frac{\pi}{L}, \frac{\pi}{L}\right]$, when $K_1 < K_2$. It is worth noting that these amplitudes cannot be zero for any value of the wave number q.

2.3. Continuum Limit

In the long wavelength limit, $\delta_{\pm}^{(j)} \to \mp ik_j a$. For large values of n and p, the dispersion relation Equations (9) or (10) reduces to the known expression [15]:

$$\cos qL = \cos k_1 d_1 \cos k_2 d_2 - \frac{1}{2}\left(\frac{1}{F} + F\right)\sin k_1 d_1 \sin k_2 d_2 \tag{15}$$

In Equation (15), we define $F = \frac{k_1 K_1}{k_2 K_2}$. The solutions for the amplitudes are addressed separately in the next subsection.

2.4. Amplitudes of the Displacement Field

To find the amplitudes, we use the transfer matrix method. Equation (8) can be rewritten as:

$$\begin{pmatrix} 1 & 1 \\ f\delta_-^{(1)} & f\delta_+^{(1)} \end{pmatrix}\begin{pmatrix} A_+^N \\ A_-^N \end{pmatrix} = \begin{pmatrix} \alpha_2 & \beta_2 \\ \alpha_2\delta_-^{(2)} & \beta_2\delta_+^{(2)} \end{pmatrix}\begin{pmatrix} B_+^{N-1} \\ B_-^{N-1} \end{pmatrix} \tag{16a}$$

$$\begin{pmatrix} \alpha_1 & \beta_1 \\ f\alpha_1\delta_-^{(1)} & f\beta_1\delta_+^{(1)} \end{pmatrix}\begin{pmatrix} A_+^N \\ A_-^N \end{pmatrix} = \begin{pmatrix} 1 & 1 \\ \delta_-^{(2)} & \delta_+^{(2)} \end{pmatrix}\begin{pmatrix} B_+^N \\ B_-^N \end{pmatrix} \tag{16b}$$

Since the second relation, Equation (16b), applies to the unit cell N-1, as well as cell N, it can be inverted to obtain a relation between $\begin{pmatrix} B_+^{N-1} \\ B_-^{N-1} \end{pmatrix}$ and $\begin{pmatrix} A_+^{N-1} \\ A_-^{N-1} \end{pmatrix}$. By inserting that relation into Equation (16a), we obtain the transfer matrix relating amplitudes in one unit cell to amplitudes in the neighboring cell:

$$\begin{pmatrix} A_+^N \\ A_-^N \end{pmatrix} = \begin{pmatrix} t_{11} & t_{12} \\ t_{21} & t_{22} \end{pmatrix}\begin{pmatrix} A_+^{N-1} \\ A_-^{N-1} \end{pmatrix} \tag{17}$$

The components of the transfer matrix are given by:

$$t_{11} = \frac{1}{f\left(\delta_+^{(2)} - \delta_-^{(2)}\right)\left(\delta_+^{(1)} - \delta_-^{(1)}\right)}\alpha_1\left[\left(f\delta_+^{(1)} - \delta_-^{(2)}\right)\left(\delta_+^{(2)} - f\delta_-^{(1)}\right)\alpha_2 + \left(f\delta_+^{(1)} - \delta_+^{(2)}\right)\left(-\delta_-^{(2)} + f\delta_-^{(1)}\right)\beta_2\right]$$

$$t_{12} = \frac{1}{f\left(\delta_+^{(2)} - \delta_-^{(2)}\right)\left(\delta_+^{(1)} - \delta_-^{(1)}\right)}\beta_1\left[\left(f\delta_+^{(1)} - \delta_-^{(2)}\right)\left(\delta_+^{(2)} - f\delta_+^{(1)}\right)\alpha_2 + \left(f\delta_+^{(1)} - \delta_+^{(2)}\right)\left(-\delta_-^{(2)} + f\delta_+^{(1)}\right)\beta_2\right]$$

Here, $t_{21} = t_{12}^*$ and $t_{22} = t_{11}^*$. The star stands for a complex conjugation.
Due to the periodicity of the system, solutions will take the form of Bloch waves:

$$\begin{pmatrix} A_+^N \\ A_-^N \end{pmatrix} = e^{iqL}\begin{pmatrix} A_+^{N-1} \\ A_-^{N-1} \end{pmatrix} \tag{18}$$

Combining Equations (17) and (18) leads to the eigenvalue problem [16]:

$$\left(\begin{pmatrix} t_{11} & t_{12} \\ t_{21} & t_{22} \end{pmatrix} - e^{iqL}\begin{pmatrix} 1 & 0 \\ 0 & 1 \end{pmatrix}\right)\begin{pmatrix} A_+ \\ A_- \end{pmatrix} = 0 \tag{19}$$

If e^{iqL} is an eigenvalue of the transfer matrix, then the amplitudes A_+ and A_- are given by:

$$A_+ = -t_{12} \tag{20a}$$

$$A_- = t_{11} - e^{iqL} \tag{20b}$$

The dispersion relation of Equation (9) can be rewritten as $2\cos qL = t_{11} + t_{22}$, so Equation (20b) becomes:

$$A_- = \frac{1}{2}(t_{11} - t_{22}) - i\sin qL \tag{21}$$

After a number of trigonometric and algebraic manipulations, we obtain:
[4:04 PM] Shelly Zou

$$\begin{aligned} A_- \quad &= i\Big\{\sin k_1 d_1 \cos k_2 d_2 \\ &+ \frac{1}{\left(\delta_+^{(2)} - \delta_-^{(2)}\right)\left(\delta_+^{(1)} - \delta_-^{(1)}\right)}\Big[-2\Big(f\delta_+^{(1)}\delta_-^{(1)} + \tfrac{1}{f}\delta_+^{(2)}\delta_-^{(2)}\Big) \\ &+ \left(\delta_+^{(1)} + \delta_-^{(1)}\right)\left(\delta_+^{(2)} + \delta_-^{(2)}\right)\Big]\cos k_1 d_1 \sin k_2 d_2 - \sin qL\Big\} \end{aligned} \tag{22}$$

Furthermore, the amplitude A_+^N is given by:

$$A_+ = \frac{2i}{f\left(\delta_+^{(2)} - \delta_-^{(2)}\right)\left(\delta_+^{(1)} - \delta_-^{(1)}\right)} e^{-ik_1 d_1}\left(f\delta_+^{(1)} - \delta_+^{(2)}\right)\left(f\delta_+^{(1)} - \delta_-^{(2)}\right)\sin k_2 d_2 \tag{23}$$

In the continuum limit, these amplitudes simplify to the known expressions [10]:

$$A_+ = \frac{1}{2}\left(F - \frac{1}{F}\right)\sin k_1 d_1 \sin k_2 d_2 + \frac{i}{2}\left(F - \frac{1}{F}\right)\cos k_1 d_1 \sin k_2 d_2 \tag{24a}$$

$$A_- = i\left[\sin k_1 d_1 \cos k_2 d_2 + \frac{1}{2}\left(F + \frac{1}{F}\right)\cos k_1 d_1 \sin k_2 d_2 - \sin qL\right] \tag{24b}$$

2.5. Conditions for One-Way Propagation in Infinite Superlattices

For the continuous system, we have shown [17] that if a band contains the frequency point ω_0, such that $\sin k_2 d_2 = 0$, then at $\omega_0(q_0)$ the dispersion relation becomes $\cos q_0 L = \cos(k_1 d_1 + k_2 d_2)$, $A_+ = 0$, and $A_- = i[\sin(k_1 d_1 + k_2 d_2) - \sin q_0 L]$. This condition corresponds to a Fabry–Pérot resonance of the second medium in the superlattice unit cell [13].

Since $k_1 d_1 + k_2 d_2 > 0$, the sign of q_0 determines whether A_- vanishes or not. From Equation (16b), $A_+ = 0$ and $A_- = 0$, meaning that $B_+ = 0$ and $B_- = 0$. At $\omega_0(+q_0)$, the amplitudes of the Bloch modes may be finite, while at $\omega_0(-q_0)$ the Bloch modes equal zero. This behavior was shown to be associated with the non-conventional topology of the Bloch modes of the continuous superlattice [18]. The Berry connection undergoes a π jump at q_0, where the amplitudes vanish. The dispersion branches supporting zero-amplitude modes in the band structure of the superlattice exhibit a π Berry phase [18].

This argument also extends to a discrete superlattice with $p > 1$ in the following manner. Let us first find expressions for the eigenvalues of the transfer matrix. These eigenvalues are solutions of the equation $\lambda^2 - \lambda\left(t_{11} + t_{11}^*\right) + t_{11}t_{11}^* - t_{12}t_{12}^* = 0$. The Eigen values are given by:

$$\lambda = \frac{1}{2}(t_{11} + t_{11}^*) \pm \frac{1}{2}\sqrt{\left(t_{11} - t_{11}^*\right)^2 + 4t_{12}t_{12}^*} \tag{25}$$

For vibrational modes to be Bloch waves, we require $\lambda \propto e^{\pm iqL}$. According to Equation (23), $A_+ = -t_{12} = 0$ when $\sin k_2 d_2 = 0$. In that case, the eigenvalues reduce to:

$$\lambda = \frac{1}{2}(t_{11} + t_{11}^*) \pm \frac{1}{2}|t_{11} - t_{11}^*| \tag{26}$$

or:

$$\lambda = Real(t_{11}) \pm i|Imag(t_{11})| \tag{27}$$

where *Real* and *Imag* stand for the real and imaginary parts.

The condition for the discrete superlattice to support Bloch waves takes the form of $Real(t_{11}) \pm |Imag(t_{11})| = \cos qL \pm i\sin qL$. This condition is met only for a wave number q located on one side of the Brillouin zone, where $|Imag(t_{11})|$ can be identified as a sine function. For q on the other side of the Brillouin zone, $|Imag(t_{11})|$ is identifiable to minus one times a sine function, which has the opposite sign of $\sin qL$. In other words, λ does not span the same region of the unit circle in the complex plane as $e^{\pm iqL}$. Under this condition, Equation (20b) leads to $A_- = 0$ on one side of the Brillouin zone but $A_- \neq 0$ on the other side. $B_+ = 0$ and $B_- = 0$ on the side of the Brillouin zone, where $A_+ = 0$ and $A_- = 0$. This result indicates that the two counterpropagating eigenmodes have different modal structures with defined handedness levels, which can be interpreted as a pseudo-spin associated with the propagation direction. In the present scenario, only one pseudo-spin state is allowed to propagate in the lattice in a specific direction, associated with spin momentum locking.

It is interesting to note that for the SSH model ($n = p = 1$), $\sin k_2 d_2 = \sin k_2 a$, and since in the denominator of Equation (23) the quantity $\left(\delta_+^{(2)} - \delta_-^{(2)}\right) \propto \sin k_2 a$, both terms cancel each other; A_+ cannot vanish anymore at $\sin k_2(d_2 = a) = 0$. The component of the transfer matrix $t_{12} \neq 0$ for the SSH system. Therefore, the SSH model does not lead to zero-amplitude Bloch modes, as was noted at the end of Section 2.2. This is also true for a superlattice with a segment of harmonic lattice 1 extending beyond one lattice spacing but with a segment of harmonic lattice 2 limited to one lattice spacing ($n > 1$ and $p = 1$). The reverse ($n = 1$ and $p > 1$) is not true, thereby illustrating the importance of the choice of origin in the topology (Berry or Zak phase) of vibrational modes in superlattices [14,18].

From a physical point of view, if $\lambda \neq e^{\pm iqL}$ in one region of q, the only way the displacement can take the form of a Bloch wave with plane wave factor e^{iqNL} over the entire Brillouin zone (for all, q):

$$u_{A,m}^N = e^{iqNL}\left(A_+ e^{ik_1 ma} + A_- e^{-ik_1 ma}\right)e^{i\omega t} \tag{28a}$$

$$u_{B,l}^N = e^{iqNL}\left(B_+ e^{ik_2 la} + B_- e^{-ik_2 la}\right)e^{i\omega t} \tag{28b}$$

is by setting the terms in parentheses to zero. For any value of m or l, this implies $A_\pm = 0$ and $B_\pm = 0$.

2.6. Reciprocity Condition

Reciprocity implies that the signal received by a detector emitted by a vibration source remains the same upon the interchange of the source and the receiver. Since the considered system is linear, time-invariant, and bias-free, we expect reciprocity to be satisfied. In order to investigate reciprocity in the one-way propagation scenario, we focus on the continuum limit of the superlattice. We consider a finite continuous superlattice sandwiched between a source layer "S" and a detection layer "D" with impedances that may differ from those of materials 1 and 2. We calculate the transmission coefficient of the finite superlattice using transfer matrices, as is achieved in [19]. The transmission coefficient is given by:

$$T = \frac{4\frac{Z_D}{Z_S}}{\left(\frac{Z_D}{Z_1}b - \frac{Z_1}{Z_S}c\right)^2 + \left(d + \frac{Z_D}{Z_S}a\right)^2} \tag{29}$$

where:

$$a = \frac{\lambda - \mu}{2}\frac{\sin N\theta}{\sin\theta} + \cos N\theta$$

$$b = \sigma \frac{\sin N\theta}{\sin \theta}$$

$$c = \zeta \frac{\sin N\theta}{\sin \theta}$$

$$d = -\frac{\lambda - \mu}{2} \frac{\sin N\theta}{\sin \theta} + \cos N\theta$$

In these equations, we have:

$$\lambda = \cos k_1 d_1 \cos k_2 d_2 - F \sin k_1 d_1 \sin k_2 d_2$$

$$\mu = \cos k_1 d_1 \cos k_2 d_2 - \frac{1}{F} \sin k_1 d_1 \sin k_2 d_2$$

$$\sigma = \sin k_1 d_1 \cos k_2 d_2 + F \cos k_1 d_1 \sin k_2 d_2$$

$$\zeta = -\sin k_1 d_1 \cos k_2 d_2 - \frac{1}{F} \cos k_1 d_1 \sin k_2 d_2$$

and $\cos\theta = \frac{\lambda+\mu}{2}$. N is the number of unit cells in the superlattice. In Equation (29), Z_1, Z_D, and Z_S are the impedances of the type 1, detection, and source layers, which are chosen to be equal for illustrative purposes; however, varying Z_D and Z_S will change the results quantitively but not qualitatively. Here, instead of interchanging the source and detector, we swap media 1 and 2 by interchanging the indices 1 and 2 in Equation (29). In the long wavelength limit, we have $k_1 = \frac{\omega}{c_1}$ and $k_2 = \frac{\omega}{c_2}$, as well as $c_1 = a\sqrt{K_1}$ and $c_2 = a\sqrt{K_2}$. In Figure 2, we present the transmission coefficient as a function of the frequency for two superlattices.

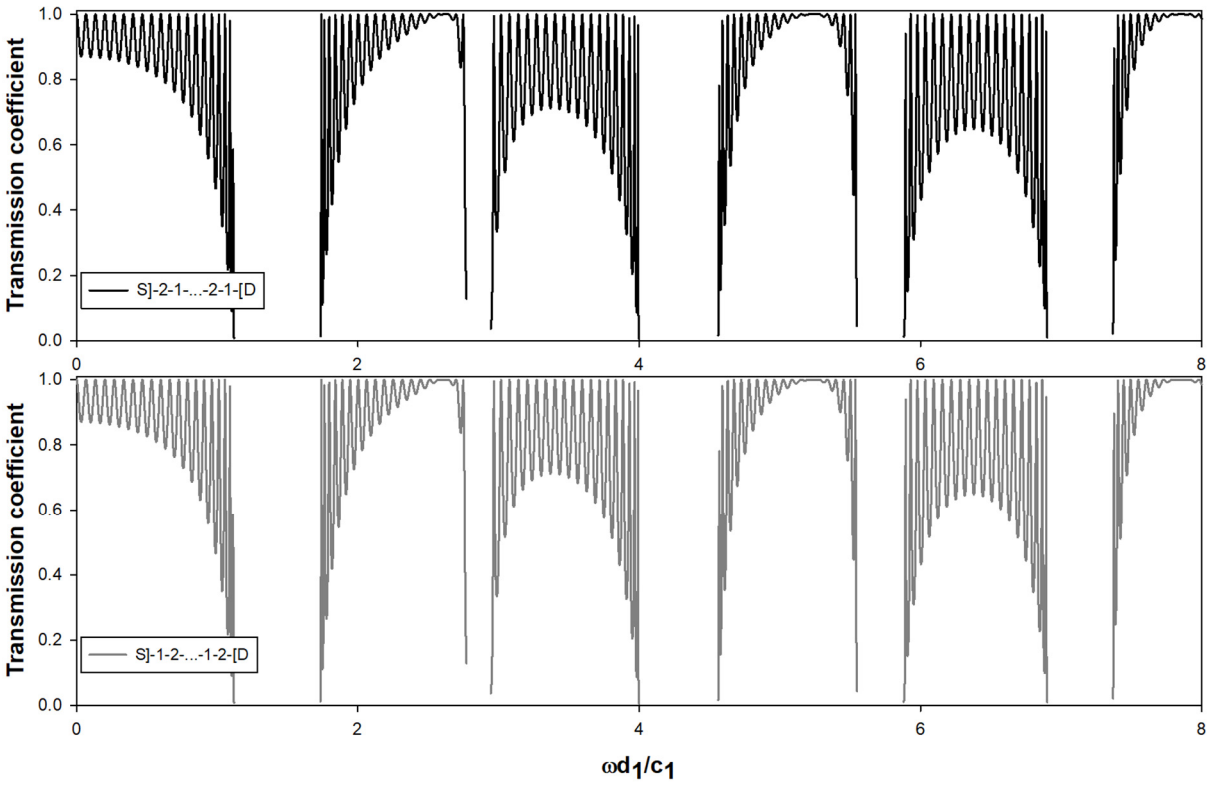

Figure 2. Transmission coefficient T, corresponding to the first 6 bands of two finite superlattices, with N = 20 as a function of the frequency for (a) $Z_D = Z_S = Z_1$. The two superlattices are related by an interchange of layer indices 1 and 2, which is equivalent to interchanging the source S and detector D. We have also chosen $k_2 d_2 = 1.2 k_1 d_1$. Each band supports 20 resonances, corresponding to the number of periods of the finite superlattice, N.

The two transmission coefficients are identical for all frequencies, confirming that reciprocity is achieved. In Figure 2, the gaps correspond to the usual Bragg scattering. These gaps arise when $\left|\frac{\lambda+\mu}{2}\right| > 1$, which corresponds to non-propagative modes.

Each band is composed of N resonances. We also note that the lower envelopes of the transmission coefficient of the 2nd and 4th transmission bands are asymmetric, while the 1st, 3rd, and 5th bands, which have conventional topologies, exhibit a more symmetrical behavior. We note in Figure 3a that the lower envelope of the transmission coefficient of the second band approaches one near $\frac{\omega}{c_1}d_1 = 2.618$ (that is, $k_2d_2 = 1.2 \times 2.618 = \pi$, which corresponds to the condition $\sin k_2d_2 = 0$). The amplitude of the backward-propagating wave equals zero under this condition. The same condition is satisfied for the fourth band $\frac{\omega}{c_1}d_1 = 5.236$, where $k_2d_2 = 2\pi$. This behavior arises for the even-numbered bands in the transmission spectrum. These bands are known to correspond to dispersion bands of the infinite superlattice with a non-conventional topology, for which the Berry or Zak phase is equal to π. The odd-numbered bands are associated with conventional topologies and zero Berry or Zak phases. This type of asymmetry in the transmission of topologically non-conventional bands has been observed theoretically for electronic waves in finite semiconductor superlattices [20] and electromagnetic superlattices [18].

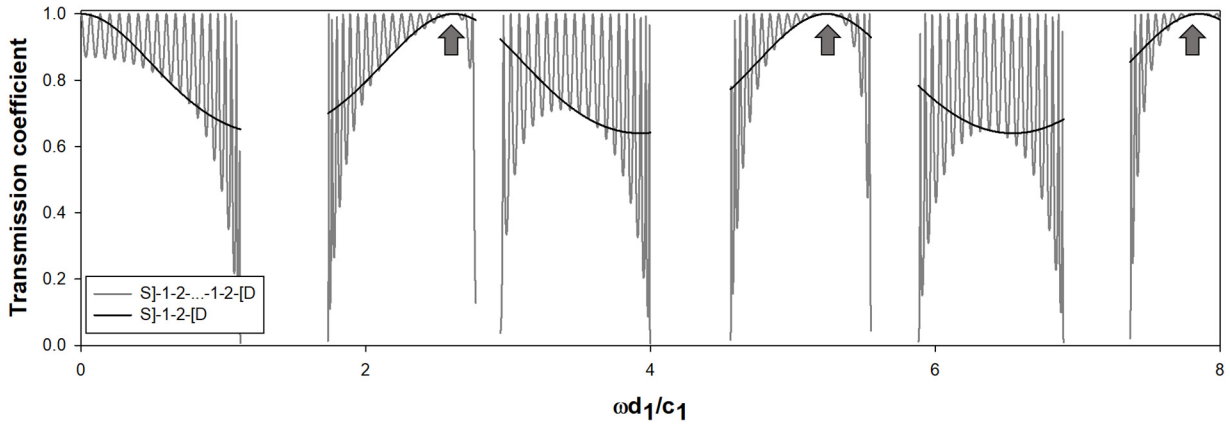

Figure 3. The same scheme as in Figure 1. The black solid line is for a single unit cell $N = 1$, sandwiched between the source and the detector. The arrows mark the location where $\sin k_2d_2 = 0$.

In Figure 3, we can clearly see that the asymmetry in the dispersion of the transmission of the even-numbered bands is associated with the Fabry–Pérot resonance condition of medium 2 in a single unit cell, $\sin k_2d_2 = 0$, where the transmission coefficient is equal to one. This is exactly the condition for which, in an infinite superlattice, spin-selective one-way propagation occurs, as imposed by the requirement that the waves take the form of Bloch waves, i.e., the waves satisfy translational invariance. Note that for a single unit cell, gaps exist that again correspond to the condition $\left|\frac{\lambda+\mu}{2}\right| > 1$.

To shed more light on the relationship between the behaviors of the finite system and the infinite system, below we give the transfer matrix across one unit cell derived in [19]. The displacement field in the two media 1 and 2 of a unit cell is expressed as a general ansatz formed as a linear combination of transmitted and reflected waves:

$$U_1(x) = \left(A_+e^{ik_1x} + A_-e^{-ik_1x}\right)e^{i\omega t} \tag{30a}$$

$$U_2(x) = \left(B_+e^{ik_2x} + B_-e^{-ik_2x}\right)e^{i\omega t} \tag{30b}$$

Here, x is the coordinate along the direction perpendicular to the layers forming the superlattice. There is no specific constraint on the form of the amplitudes A_+, A_-, B_+, and B_-.

The stress is expressed as:

$$S_1(x) = i\omega Z_1\left(A_+e^{ik_1x} - A_-e^{-ik_1x}\right)e^{i\omega t} \tag{31a}$$

$$S_2(x) = i\omega Z_2\left(B_+e^{ik_2x} - B_-e^{-ik_2x}\right)e^{i\omega t} \tag{31b}$$

These definitions allow us to introduce the two-component vector for j = 1, 2:

$$\boldsymbol{W}_j(x) = \begin{pmatrix} U_j(x) \\ S_j(x) \end{pmatrix} = \begin{pmatrix} e^{ik_jx} & e^{-ik_jx} \\ i\omega Z_j e^{ik_jx} & -i\omega Z_j e^{-ik_jx} \end{pmatrix} \begin{pmatrix} A_+ \text{ or } B_+ \\ A_- \text{or } B_- \end{pmatrix} \tag{32}$$

Here, we define $\boldsymbol{H}_j(x) = \begin{pmatrix} e^{ik_jx} & e^{-ik_jx} \\ i\omega Z_j e^{ik_jx} & -i\omega Z_j e^{-ik_jx} \end{pmatrix}$. In a stack of unit cells, using the conditions of the continuity of displacement and stress, one can relate $W_1(x = d_1 + d_2)$ right after a unit cell to $W_1(x = 0)$ right before a unit cell using the following relation:

$$\boldsymbol{W}_1(x = L = d_1 + d_2) = \boldsymbol{M}\boldsymbol{W}_1(x = 0) \tag{33}$$

where:

$$\boldsymbol{M} = \begin{pmatrix} \lambda & \frac{1}{Z_1\omega}\sigma \\ Z_1\omega\zeta & \mu \end{pmatrix} \tag{34}$$

The symbol in Equation (34) was defined earlier. We remark that there is no constraint imposed on the ansatz of Equation (30a,b). For the periodic infinite superlattice and a unit cell labelled, N, we must use a continuous version of the Bloch wave ansatz given by Equation (28a,b):

$$U_1^N(x) = e^{iqNL}\left(A_+^p e^{ik_1(x-NL)} + A_-^p e^{-ik_1(x-NL)}\right)e^{i\omega t} \text{ for } NL < x < NL + d_1 \tag{35a}$$

$$U_2^N(x) = e^{iqNL}\left(B_+^p e^{ik_1(x-NL-d_1)} + B_-^p e^{-ik_1(x-NL-d_1)}\right)e^{i\omega t} \text{ for } NL + d_1 < x < (N+1)L \tag{35b}$$

This ansatz achieves translational periodicity, as it represents Bloch waves. In Equation (35a,b), the upper script "p" stands for periodic. This is necessary as the periodicity redefines the amplitude parameters. Comparing Equation (30a,b) and Equation (35a,b), we can establish constraints that would be imposed by translational invariance on the parameters A_+, A_-, B_+, and B_-, namely:

$$\begin{pmatrix} A_+ \\ A_- \end{pmatrix}_N = \begin{pmatrix} e^{-ik_1NL} & 0 \\ 0 & e^{ik_1NL} \end{pmatrix} e^{iqNL} \begin{pmatrix} A_+^p \\ A_-^p \end{pmatrix} \tag{36a}$$

$$\begin{pmatrix} B_+ \\ B_- \end{pmatrix}_N = \begin{pmatrix} e^{-ik_1(NL+d_1)} & 0 \\ 0 & e^{ik_1(NL+d_1)} \end{pmatrix} e^{iqNL} \begin{pmatrix} B_+^p \\ B_-^p \end{pmatrix} \tag{36b}$$

These are actually unitary transformations, which rotate the representation amplitudes of the periodic system into the representation of the amplitudes in Equation (30a,b).

By using Equation (32) and inserting Equation (36a,b) into Equation (33), i.e., N = 1 for the left hand side of the equal sign and N = 0 for the right hand side, one obtains the following relation:

$$\left(\begin{pmatrix} t_{11} & t_{12} \\ t_{21} & t_{22} \end{pmatrix} - e^{iqL}\begin{pmatrix} 1 & 0 \\ 0 & 1 \end{pmatrix}\right)\begin{pmatrix} A_+^p \\ A_-^p \end{pmatrix} = 0. \tag{37}$$

with:

$$\boldsymbol{T} = \begin{pmatrix} t_{11} & t_{12} \\ t_{21} & t_{22} \end{pmatrix} = \boldsymbol{H}_1^{-1}(0)\boldsymbol{M}\boldsymbol{H}_1(0) \tag{38}$$

After some algebraic manipulation, we find:

$$t_{11} = \frac{\lambda+\mu}{2} + i\frac{\sigma-\zeta}{2},\ t_{12} = \frac{\lambda-\mu}{2} + i\frac{\sigma+\zeta}{2},\ \text{and } t_{21} = t_{12}^{*} \text{ and } t_{22} = t_{11}^{*}.$$

One can verify algebraically that Equation (37) is identical to Equation (19). We can also observe that the determinants of the unimodular matrices M and $\boldsymbol{T}$ are identical and given by $\lambda\mu - \sigma\zeta = 1$. When solving the eigenvalues, ε of the matrix $\boldsymbol{M}$ gives a characteristic equation of $\varepsilon^2 - (\lambda+\mu) + 1 = 0$. The finite superlattice takes a propagative eigenmode when $\left|\frac{\lambda+\mu}{2}\right| \leq 1$. By setting $\cos\theta = \frac{\lambda+\mu}{2}$, the characteristic equation takes the form of the dispersion relation of the infinite superlattice (Equation (10)) in the limits of the long wavelength, provided one identifies θ with qL. Equations (37) and (19) achieve translational invariance and lead to one-way propagation (zero amplitudes for q < 0 and non-zero amplitudes for q > 0) when $\sin k_2 d_2 = 0$. When dealing with the finite superlattice, the unconstrained matrix $\boldsymbol{M}$ is diagonalized with the eigenvalues $\varepsilon_+ = e^{i\theta}$ and $\varepsilon_- = e^{-i\theta}$, which account for forward and backward propagation and are associated with the different pseudo-spins of the eigenvectors. The diagonalized matrix is then brought to the power N to calculate the transmission coefficient of Equation (29) for the finite lattice with N unit cells. The wave function of the finite superlattice will try to approach the Bloch wave solutions. Under the condition $\sin k_2 d_2 = 0$, the approximate Bloch wave will make the contribution of the backward-propagating wave (i.e., $e^{-i\theta}$) small compared to the forward wave, thereby leading to high values of the transmission coefficient. One-way propagation in the infinite superlattice arises from the combined effects of the constraint of the translational invariance of the wave function and of a Fabry–Pérot resonance condition in the superlattice unit cell.

3. Conclusions

One-dimensional discrete phononic superlattices composed of alternating segments of two different harmonic crystals exhibit Bloch modes with specified handedness, with a finite amplitude for one direction and zero amplitude for the opposite direction. By using the transfer matrix method, i.e., solving the scattering of acoustic waves by the superlattice, we showed that the one-way transport nature of these eigenwaves arises from the periodicity of the system, even when the eigenvalues of the transfer matrix do not span the complete unit circle in the complex plane. The one-way propagation behavior of the discrete superlattice approaches that of a continuous superlattice in the long wavelength limits. A necessary condition for one-way propagation in our superlattice model is that the second harmonic crystal segment possesses a spatial extent that exceeds the lattice parameter. This condition enables Fabry–Pérot-type resonances. In the limits of a superlattice composed of single lattice parameter segments, the model reduces to the SSH system, which does not exhibit one-way propagation. In this case, the eigenvalues of the transfer matrix span the complete unit circle in the complex plane and allow Bloch modes with non-zero amplitude to exist over the entire Brillouin zone. By comparing an infinite superlattice and a finite superlattice in the long wavelength limits, we also showed that reciprocity is always achieved. One-way propagation in the infinite superlattice results from the combined effects of translational periodicity, the non-trivial handedness of the associated eigenvector associated with a pseudo-spin, and the Fabry–Pérot resonances of the second medium in the unit cell of the binary superlattice. Phononic superlattices supporting topologically protected acoustic or elastic waves that avoid back-reflections may provide attractive solutions for designing low-loss devices such as bulk or surface acoustic wave devices for telecommunication systems [21]. Another application of current interest is the use of one-way propagation for the management of thermal phonons. Specifically, recent advances in this context have been reported for phonon focusing [22], thermal switching [23], and thermal barriers [24]. Furthermore, binary superlattices that can be manufactured using thin-film deposition methods [25] or colloid-assembled nanocrystal superlattices [26] can serve as platforms for phonon engineering. These offer viable platforms for the experimental investigation of the effects discussed herein.

Author Contributions: Conceptualization, P.A.D. and K.R.; methodology, P.A.D., K.R., A.K. and A.A..; formal analysis, P.A.D., K.R., A.K. and A.A..; writing—original draft preparation, P.A.D. and K.R.; writing—review and editing, A.K. and A.A.; funding acquisition, P.A.D., K.R., A.K. and A.A. All authors have read and agreed to the published version of the manuscript.

Funding: This research was funded by the US National Science Foundation (NSF) grant #2242925 through the Science and Technology Center New Frontiers of Sound (NewFoS).

Data Availability Statement: The data presented in this study are available on request from the corresponding author.

Conflicts of Interest: The authors declare no conflict of interest.

References

1. Rasmussen, C.; Quan, L.; Alù, A. Acoustic nonreciprocity. *J. Appl. Phys.* **2021**, *129*, 210903. [CrossRef]
2. Nassar, H.; Yousefzadeh, B.; Fleury, R.; Ruzzene, M.; Alù, A.; Daraio, C.; Norris, A.N.; Huang, G.; Haberman, M.R. Nonreciprocity in acoustic and elastic materials. *Nat. Rev. Mater.* **2020**, *5*, 667. [CrossRef]
3. Wang, P.; Lu, L.; Bertoldi, K. Topological phononic crystals with one-way elastic edge waves. *Phys. Rev. Lett.* **2015**, *115*, 104302. [CrossRef]
4. Nadkarni, N.; Arrieta, A.F.; Chong, C.; Kochmann, D.M.; Daraio, C. Unidirectional transition waves in bistable lattices. *Phys. Rev. Lett.* **2016**, *116*, 244501. [CrossRef] [PubMed]
5. Swinteck, N.; Matsuo, S.; Runge, K.; Vasseur, J.O.; Lucas, P.; Deymier, P.A. Bulk elastic waves with unidirectional backscattering-immune topological states in a time-dependent superlattice. *J. Appl. Phys.* **2015**, *118*, 063103. [CrossRef]
6. Nassar, H.; Chen, H.; Norris, A.N.; Haberman, M.R.; Huang, G.L. Non-reciprocal wave propagation in modulated elastic metamaterials. *Proc. R. Soc. A* **2017**, *473*, 20170188. [CrossRef]
7. Nassar, H.; Xu, X.C.; Norris, A.N.; Huang, G.L. Modulated phononic crystals: Non-reciprocal wave propagation and Willis materials. *J. Mech. Phys. Solids* **2017**, *101*, 10–29. [CrossRef]
8. Khanikaev, A.B.; Fleury, R.; Mousavi, S.H.; Alù, A. Topologically robust sound propagation in an angular-momentum-biased graphene-like resonator lattice. *Nat. Commun.* **2015**, *6*, 8260. [CrossRef]
9. Fleury, R.; Khanikaev, A.B.; Alù, A. Floquet topological insulators for sound. *Nat. Commun.* **2016**, *7*, 11744. [CrossRef]
10. Deymier, P.A.; Runge, K.; Vasseur, J.O. Geometric phase and topology of elastic oscillations and vibrations in model systems: Harmonic oscillator and superlattice. *AIP Adv.* **2016**, *6*, 121801. [CrossRef]
11. Su, W.P.; Schrieffer, J.R.; Heeger, A.J. Solitons in Polyacetylene. *Phys. Rev. Lett.* **1979**, *42*, 1698. [CrossRef]
12. Huang, H.; Chen, J.; Huo, S. Recent advances in topological elastic metamaterials. *J. Phys. Condens. Matter* **2021**, *33*, 503002. [CrossRef] [PubMed]
13. Pérot, A.; Fabry, C. On the application of interference phenomena to the solution of various problems of spectroscopy and metrology. *Astrophys. J.* **1899**, *9*, 87. [CrossRef]
14. Hasan, M.A.; Calderin, L.; Runge, K.; Deymier, P.A. Spectral Analysis of Amplitudes and Phases of Lattice Vibrations: Topological Applications. *J. Acoust. Soc. Am.* **2019**, *146*, 748. [CrossRef] [PubMed]
15. Camley, R.E.; Djafari-Rouhani, B.; Dobrzynski, L.; Maradudin, A.A. Transverse elastic waves in periodically layered infinite and semi-infinite media. *Phys. Rev. B* **1983**, *27*, 7318. [CrossRef]
16. Yariv, A.; Yeh, P. *Optical Waves in Crystals: Propagation and Control of Laser Radiation*; Wiley: New York, NY, USA, 1984.
17. Deymier, P.A.; Runge, K. *Sound Topology, Duality, Coherence and Wave-Mixing: An Introduction to the Emerging New Science of Sound*; Springer Series in Solid-State Sciences; Springer: Berlin/Heidelberg, Germany, 2017; Volume 188.
18. Xiao, M.; Zhang, Z.Q.; Chan, C.T. Surface impedance and bulk band geometric phases in one-dimensional systems. *Phys. Rev. X* **2014**, *4*, 021017. [CrossRef]
19. Mizuno, S.; Tamura, S.-I. Theory of acoustic-phonon transmission in finite-size superlattice systems. *Phys. Rev. B* **1992**, *45*, 734. [CrossRef]
20. Luo, X.; Shi, J.; Zhang, Y.; Niu, Z.; Miao, D.; Mi, H.; Huang, W. Filtering electrons by mode coupling in finite semiconductor superlattices. *Sci. Rep.* **2022**, *12*, 7502. [CrossRef]
21. Deymier, P.A.; Runge, K. One-way propagation of topologically non-conventional bulk transverse elastic waves in infinite and finite superlattices: Application to low-loss acoustic wave devices. *Appl. Phys. Lett.* **2023**, *123*, 012202. [CrossRef]
22. Anufriev, R.; Ramiere, A.; Maire, J.; Nomura, M. Heat guiding and focusing using ballistic phonon transport in phononic nanostructures. *Nat. Commun.* **2017**, *8*, 15505. [CrossRef]
23. Ishibe, T.; Kaneko, T.; Uematsu, Y.; Sato-Akaba, H.; Komura, M.; Iyoda, T.; Nakamura, Y. Tunable Thermal Switch via Order-Order Transition in Liquid Crystalline Block Copolymer. *Nano Lett.* **2022**, *22*, 6105. [CrossRef]
24. Ahn, C.; Fong, S.W.; Kim, Y.; Lee, S.; Sood, A.; Neumann, C.M.; Asheghi, M.; Goodson, K.E.; Pop, E.; Wong, H.-S.P. Energy-Efficient Phase-Change Memory with Graphene as a Thermal Barrier. *Nano Lett.* **2015**, *15*, 6809. [CrossRef]

25. Kothari, K.; Malhotra, A.; Maldovan, M. Cross-plane heat conduction in III-V semiconductor superlattices. *J. Phys. Condens. Matter* **2019**, *31*, 345301. [CrossRef]
26. Yazdani, N.; Jansen, M.; Bozyigit, D.; Lin, W.M.M.; Volk, S.; Yarema, O.; Yarema, M.; Juranyi, F.; Huber, S.D.; Wood, V. Nanocrystal superlattices as phonon-engineered solids and acoustic metamaterials. *Nat. Commun.* **2019**, *10*, 4236. [CrossRef]